

Wild swarms of midges linger at the edge of an ordering phase transition

Alessandro Attanasi^{*,‡}, Andrea Cavagna^{*,‡}, Lorenzo Del Castello^{*,‡}, Irene Giardina^{*,‡}, Stefania Melillo^{*,‡}, Leonardo Parisi^{*,§}, Oliver Pohl^{*,‡}, Bruno Rossaro[‡], Edward Shen^{*,‡}, Edmondo Silvestri^{*,†}, Massimiliano Viale^{*,‡}

^{*} *Istituto Sistemi Complessi, Consiglio Nazionale delle Ricerche, UOS Sapienza, 00185 Rome, Italy*

[‡] *Dipartimento di Fisica, Università Sapienza, 00185 Rome, Italy*

[§] *Dipartimento di Informatica, Università Sapienza, 00198 Rome, Italy*

[†] *Dipartimento di Fisica, Università di Roma 3, 00146 Rome, Italy and*

[‡] *Dipartimento di Scienze per gli Alimenti la Nutrizione e l'Ambiente, Università degli Studi di Milano, 20133 Milano, Italy*

The most notable hallmark of collective behaviour in biological systems is the emergence of order: individuals polarize their state, giving the stunning impression that the group behaves as one. Mating swarms of mosquitoes and midges, however, do not display global order and it is therefore unclear whether swarms are a true instance of collective behaviour or a mere epiphenomenon of the independent response of each insect to an environmental stimulus. Here, we experimentally study wild swarms of midges by measuring their susceptibility, namely the capability to collectively respond to an external perturbation. The susceptibility is way larger than that of a noninteracting system, indicating the presence of strong coordination, and it increases sharply with the swarm density, a distinctive mark of an incipient ordering phase transition. We find that swarms live at the near-critical edge of this transition, suggesting that their size and density are tuned to maximize collective response.

Intuition tells us that a system displays collective behaviour when all individuals spontaneously do the same thing, whatever this thing may be. We surely detect collective behaviour when all birds in a flock fly in the same direction and turn at the same time [1], as well as when all spins in a magnet align, giving rise to a macroscopic magnetization [2, 3]. On the other hand, we would not say that there is much collective behaviour going on in a gas, despite the large number of molecules. The concept of collective behaviour seems therefore closely linked to that of emergent collective order and indeed explaining how order spontaneously arises from the inter-individual interactions has been the major focus of interest in the field [4–6].

The case of insect swarms is tricky in this respect. Several species in the vast taxonomic order Diptera (flies, mosquitoes, midges) form big swarms consisting largely of males, whose purpose is to attract females [7, 8]. Swarming therefore has a key reproductive function and, in some cases, relevant health implications, the obvious, but not unique, example being that of the malaria mosquito, *Anopheles gambiae* [9–11]. It is well-known that swarms form in proximity of some visual marker, like a water pool, or a street lamp [7]. Swarming insects seem to independently fly around this marker, without paying much attention to each other (see SM-Video 1). For this reason, the question of whether swarms behave as a collective is debated [4, 12]. It has been suggested that in Diptera there is no interaction between individuals within the swarm and therefore no collective behaviour at all [13, 14]. Although local coordination between nearest neighbors has been observed [15, 16], it remains controversial whether and to what extent collective patterns emerge over the scale of the whole group. Clarifying this issue is a central goal in swarms containment [17, 18]. In absence of quantitative evidence telling

the contrary, the hypothesis that external factors are the sole cause of swarming and that no genuine collective behaviour is present, is by far the simplest explanation.

Physics, however, warns us that we must be careful in identifying collective behaviour with collective order. There are systems displaying important collective effects both in their ordered *and* in their disordered phase. The classic example is that of a ferromagnet: the collective response slightly above the critical temperature T_c , i.e. the temperature below which a spontaneous magnetization emerges, is as strong as slightly below T_c , in the ordered phase. In fact, once below the critical temperature, increasing the amount of order *lowers* the collective response [2, 3]. Hence, although certainly one of its most visible manifestations, emergent order is not necessarily the best probe of collective behaviour.

RESULTS

Experiments. We perform an experimental study of wild swarms of midges in the field (Diptera:Chironomidae and Diptera:Ceratopogonidae - see Methods). We reconstruct the 3d trajectories of individual insects within swarms ranging in size from 100 to 600 individuals (see Fig.1a and SM-Table 1). Our apparatus does not perturb the swarms in any way. A sample 3d reconstruction of a swarm is shown in Fig.1a and in SM-Video 2. Compared to previous field [11, 15, 19] and lab [20] studies, the present work is the most extensive experimental study of swarming insects in three dimensions to date.

Order parameters. Swarms are in a disordered phase. The standard order parameter is the polarization, $\Phi = |(1/N) \sum_i \vec{v}_i / v_i|$, where N is the number of midges in the swarm and \vec{v}_i is the velocity of insect i .

The polarization measures the degree of alignment of the directions of motion (its maximum value is 1). The average polarization over all swarms is quite small, $\Phi \sim 0.21$ (see SM-Table 1). Rotational and dilatational order parameters (see Methods) have values in the same range. As a reference, in starling flocks $\Phi \sim 0.97$ [21]. The time series, however, shows that the order parameters do have strong fluctuations, during which their value become significantly larger than that of an uncorrelated system (Fig.1b). These large fluctuations are a first hint that nontrivial correlations are present in natural swarms.

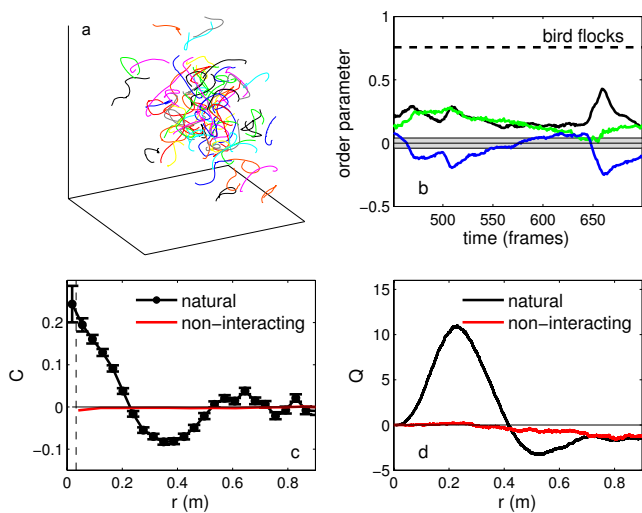


FIG. 1. **Swarms are strongly correlated.** **a:** 3d reconstruction of a swarm. Individual trajectories are visualized for a short time and for a small swarm, to avoid visual overcrowding (see also SM-Video 1 and 2). **b:** Order parameters as a function of time (1 frame = 1/170sec). Polarization (black), rotation (green) and dilatation (blue). The dashed line is the typical polarization of bird flocks. The grey band around zero is the expected amplitude of the fluctuations in a completely uncorrelated system, $\pm 1/\sqrt{N}$. The order parameters have strong fluctuations, suggesting that swarms are correlated. However, the value of the order parameters is never large for long interval of time. Swarms are, overall, in a disordered phase. **c:** The connected correlation function, $C(r)$, measures to what extent the velocity fluctuations of a midge are correlated to the velocity fluctuations of midges at distance r from it. The point where the correlation first crosses zero, r_0 , gives an estimate of the correlation length. Black: correlation function in a natural swarm (20120917_A3) at a single instant of time. The dashed vertical line marks the average nearest neighbour distance, r_1 , in this swarm. We clearly see that $r_0 \gg r_1$. Red: correlation function in a synthetic ‘swarm’ of non-interacting particles (NHS). **d:** Volume integral of the correlation function, $Q(r)$. This function reaches a maximum in correspondence with r_0 . The value of the integrated correlation at its maximum, $\chi \equiv Q(r_0)$, is the susceptibility, which is directly connected to the collective response of the system. Black: same natural swarms as in c. Red: NHS.

Correlation. The connected correlation function, $C(r)$, measures to what extent the change in behaviour

of individual i is correlated to that of j at distance r (see SM-Section I). Correlation can be measured for different quantities, but in the case of midges, as with birds and other moving animals, the principal quantity of interest is the velocity. Correlation is the most accessible sign of the presence of interaction between the members of a group. The absence of interaction implies the absence of correlation. Conversely, the presence of correlation implies the presence of interaction [22]. The definition of the correlation function is the following,

$$C(r) = \frac{\sum_{i \neq j}^N \delta \vec{\varphi}_i \cdot \delta \vec{\varphi}_j \delta(r - r_{ij})}{\sum_{i \neq j}^N \delta(r - r_{ij})}, \quad (1)$$

where $\delta \vec{\varphi}_i$ is the (dimensionless) velocity fluctuation of midge i , namely the difference between its full velocity and the mean motion of the swarm (see Methods). The form of $C(r)$ in natural swarms is nontrivial (Fig.1c): at short distances there is strong positive correlation, indicating that midges tend to align their velocity to that of their neighbours; then, after some negative correlation at intermediate distances, $C(r)$ relaxes to no correlation for large distances. This qualitative form is quite typical of all species analyzed (see SM-Fig. 6). The value of r_0 where the $C(r)$ crosses zero gives an estimate of the length scale over which the velocity fluctuations are correlated [21]. The average value of this correlation length over all analyzed swarms is, $r_0 \sim 0.19$ m. This value is about 4 times larger than the nearest neighbours distance, whose average over all swarms is, $r_1 \sim 0.05$ m (see SM-Table 1). Previous works noticed the existence of pairing maneuvers and flight-path coordination between nearest neighbours [4, 15, 16]. Our results, however, indicate that midges influence each other’s motion far beyond their nearest neighbour (Fig.1c), showing that coordination occurs at a truly collective level.

Susceptibility. The collective response of the swarm depends crucially on two factors: how distant in space the behavioural coherence of midges extends (spatial span of the correlation) and how strong this coherence is (intensity of the correlation). To take into account these two factors we calculate the volume integral of the correlation, which combines them into one single quantity,

$$Q(r) = \frac{1}{N} \sum_{i \neq j}^N \delta \vec{\varphi}_i \cdot \delta \vec{\varphi}_j \theta(r - r_{ij}). \quad (2)$$

This function reaches a maximum for $r = r_0$ (see Fig.1d). This maximum, $\chi \equiv Q(r_0)$, is a measure of the total amount of correlation present in the system. In statistical physics χ is called susceptibility [22, 23] and it is directly related to the collective response of the system to external perturbations (see SM-Section II). In order to judge how large is χ , we need an effective zero value for it. Following Okubo [4] (but see also [20] and [16]), we simulate a ‘swarm’ of noninteracting particles performing a random walk in a three-dimensional har-

monic potential (see Methods). Visually, the group behaviour of this NHS (Noninteracting Harmonic Swarm) looks very similar to that of a real swarm: all ‘midges’ fly around the marker, but the group lacks collective order (see SM-Video 2 and 3). This similarity, however, is deceptive. In the NHS, the susceptibility is extremely small, $\chi_{\text{NHS}} \sim 0.1$, whereas the susceptibility in natural swarms is up to 100 times larger than this non-interacting benchmark (Fig.1d). Moreover, the correlation function $C(r)$ in the NHS simply fluctuates around zero, with no spatial span, nor structure (Fig.1c). We conclude that, despite the lack of collective order, natural swarms are strongly correlated on large length scales. There exist big clusters of midges that move coherently, contributing to the ‘dancing’ visual effect of the swarm. The only way this can happen is that midges interact. What kind of interaction is that?

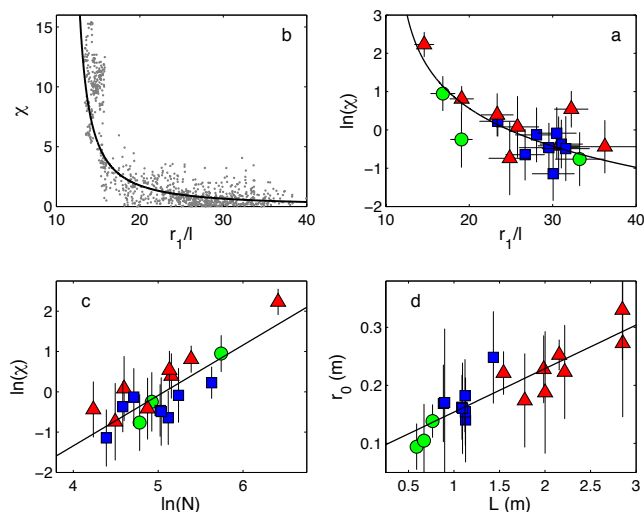


FIG. 2. **Swarms susceptibility.** **a:** Susceptibility as a function of the rescaled nearest neighbour distance, r_1/l , where l is the body length. Each point is a single time frame of a swarming event and all events are reported on the same plot (symbols are equal for all species). The sharp increase of χ with decreasing distance is at the same time a clear signature of an interaction mechanism based on metric distance and an indication of a phase transition. The full line is the best fit to equation (4), performed in semi-log scale. **b:** Logarithm of the susceptibility as a function of r_1/l . Each data point is the time average over the entire acquisition of one swarming event. Error bars are standard deviations. Species are (see SM-Table I): green circles: CS; red triangles: CA; blue squares: DF. The full line is the same as in **a**, i.e. the best fit to (4). **c:** Susceptibility as a function of the number of midges N in the swarm. There is no evident sign of saturation, suggesting that swarms are in a scaling regime. **d:** Correlation length, r_0 , as a function of the linear system size, L . Also the correlation length, consistently with the susceptibility, shows no saturation for large systems.

Metric interaction. To answer this question we note that the susceptibility, χ , increases sharply when the average nearest neighbour distance, r_1 , decreases

(Fig.2a and 2b). Denser swarms are more correlated than sparser ones. This fact strongly suggests that midges interact through a metric perceptive apparatus: the strength of the perception likely decreases with the distance, so that when midges are further apart from each other (larger r_1) the interaction is weaker and the susceptibility χ is lower. This is at variance with what happens in bird flocks: birds interact with a fixed number of neighbours, irrespective of their nearest neighbour distance r_1 [24]; such kind of topological interaction does not depend on the group density, hence the susceptibility does not depend on the nearest neighbour distance. Figure 2, on the other hand, shows that midges interact metrically, namely with all neighbours within a fixed metric range, λ . Hence, in a swarm the number of interacting neighbours increases with decreasing r_1 (increasing density), and the system becomes more correlated. A metric interaction mechanism implies that the range of the interaction is fixed by a perceptive mechanism, rather than a cognitive one, as in birds [24]. This seems reasonable, considering the significant difference between arthropods and vertebrates.

In a system ruled by metric interaction we expect all lengths to be measured in units of the perception range, λ . This implies that the natural variable for the susceptibility is the rescaled nearest neighbour distance, r_1/λ . The problem is that we are considering different species, likely to have different metric perception ranges. The simplest hypothesis we can make is that λ is proportional to the insect body length l (which we can measure), so that $\chi = \chi(r_1/l)$. This hypothesis is confirmed by the data: the susceptibility is significantly more correlated to r_1/l (P-value = 0.0004) than to r_1 (P-value = 0.07). The fact that the natural variable is r_1/l is a further indication that the interaction in swarms is based on a metric perception range.

Ordering transition. The sharp growth of the susceptibility with increasing density that we observe is a key prediction of the Vicsek model of collective motion [25]. In this model each individual tends to align its direction of motion to that of neighbours within a metric perception range λ . The model predicts a transition from a disordered phase (swarming) at high values of r_1/λ to an ordered phase (flocking) at low values of r_1/λ [25–27]. A swarming to flocking transition is also explicitly observed in model [28]. The rescaled nearest neighbour distance, $x \equiv r_1/\lambda$, is the control parameter. This transition has been experimentally observed in laboratory experiments on locusts [29], fish [30] and in observations of oceanic fish shoals [31]. In these cases, both sides of the ordering transition were observed. On the other hand, midge swarms are always quite disordered, indicating that they live in the low-density/high- x side of the transition.

In the Vicsek model the ordering transition is marked by a peak of the susceptibility, reached at a certain ‘critical’ value $x = x_{\text{max}}$ of the rescaled nearest neighbour distance (Fig.3a). This is a crucial point in the param-

eters space: here the system is about to order and the collective response of the group to an external perturbation is maximal. This value, x_{\max} , is a finite-size manifestation of the true critical point, x_c that develops for $N \rightarrow \infty$. For larger N , the position of the peak moves to the left, $x_{\max}(N) \rightarrow x_c$, and the peak becomes sharper and sharper, $\chi_{\max}(N) \rightarrow \infty$ (see [27] and SM-Section III for a discussion on the nature of the transition). If we increase the size N of the group at *fixed* value of the nearest neighbour distance x , the susceptibility χ initially grows, but then saturates for large N at its bulk value (Fig.3b). At small sizes, increasing N means adding more and more correlated individuals that respond in a coordinated way, thus enhancing the collective response of the entire group. However, when N becomes much larger than the number of correlated individuals, an increase of the size amounts to including elements that respond independently to perturbations and no longer add to the collective response of the group.

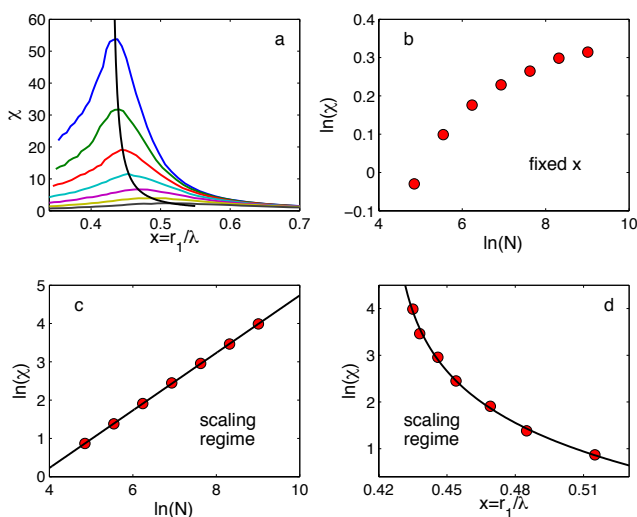


FIG. 3. **Vicsek model.** **a:** Susceptibility χ as a function of the rescaled nearest neighbour distance, $x = r_1/\lambda$, at various sizes (from grey to blue): $N = 128, 256, 512, 1024, 2048, 4096, 8192$. The maximum of χ occurs at the finite-size critical point, $x_{\max}(N)$. This maximum becomes sharper and sharper for increasing N . If we fix x and increase N , we obtain the curve in panel **b**: the susceptibility saturates for large N . This is the typical behaviour of a system far from the scaling region. On the other hand, if we stay close to the peak of the susceptibility, by tuning simultaneously x and N , we obtain that χ does not saturate for large N , panel **c**. This scaling regime is obtained by following to the line in panel **a**, which marks the true phase transition described by equation (4). The behaviour of the logarithm of χ as a function of the rescaled nearest neighbour distance is displayed in panel **d**, to be compared to the swarms data, Fig.2b.

Scaling scenario. Interestingly, this saturation of χ with N does *not* happen in natural swarms. Instead, the susceptibility scales with N up to our largest sizes

($P < 10^{-6}$ - Fig.2c). There is nothing wrong with the aforementioned explanation, though: the saturation of χ for large N should only occur at *fixed* value of the rescaled nearest neighbour distance $x = r_1/\lambda$. Swarms, however, pick up their own size and density, i.e. their own values of N and r_1/λ . The fact that $\chi \sim N$ at all sizes suggests that when N gets larger, r_1/λ decreases, as if swarms were following the peak of the susceptibility, yet remaining on the disordered side of the transition (see SM-Fig.7). This means that swarms live in a rather peculiar region of the (x, N) plane, the one defined by the relation,

$$x \gtrsim x_{\max}(N). \quad (3)$$

This is the scaling, or scale-free, region [2, 3]. Equation (3) means that a swarm is always close to the ridge of the function $\chi(x, N)$ in Fig.3a. The theory of critical phenomena [2] shows that in the scaling region, χ does not saturate with N . The theory also shows that in the scaling regime the correlation length must scale with the linear system size, $r_0 \sim L$ (see SM-Section IV). This second scaling relation too is satisfied in natural swarms (Fig.2d), similarly to what happens in bird flocks [21]. We note that to see this scaling behaviour of the susceptibility and of the correlation length one needs moderate to large groups. It would be very difficult to see this phenomenon with swarms of a few tens of individuals. This is somewhat a limitation of lab compared to field studies.

At the edge of the transition. Finite size scaling theory asserts that all pairs (x, N) belonging to the scaling regime (3), obey the equation [32–34],

$$\chi \sim \frac{1}{(x - x_c)^\gamma}, \quad x = r_1/\lambda. \quad (4)$$

Thus, in the scaling region one observes a finite- N simulacrum of the bulk phase transition. We numerically explored the scaling regime of the Vicsek model (Fig.3c and 3d) and found $x_c \equiv (r_1)_c/\lambda \sim 0.43 \pm 0.01$ and $\gamma = 1.5 \pm 0.1$. We can now use this value of γ to fit equation (4) to the swarm susceptibility data. As we already mentioned, we do not know the value of the metric perception range, λ , so we use as scaling variable r_1/l , where l is the body length. The fit works reasonably well (Fig.2b) and gives $(r_1)_c/l = 11.2 \pm 1.5$. This suggests that, if we could tune the swarms' density, there would be an ordering transition when the nearest neighbour distance between midges becomes lower than 10-12 body lengths. Notice that our most packed midges are found at about 14 body lengths from each other, not far from the predicted phase transition.

Perception range. If we make the hypothesis that the growth of the susceptibility is a universal mechanism ruled by the ordering phase transition, we have that the critical nearest neighbour distance $(r_1)_c$ in its natural units must be the same in Vicsek as in natural swarms. We conclude that, $0.43\lambda \sim 11l$, that is (including errors), $\lambda \sim 21l - 26l$. The body length of the

species we consider is in the range, $l \sim 1.2\text{mm} - 2.4\text{mm}$. This implies a perception range of a few centimeters, $\lambda \sim 2.5 - 6.0\text{cm}$. This estimate of the perception range looks reasonable once we make the hypothesis that midges interact acoustically. In [35] the male-to-male auditory response in *Chironomus annularius* (Diptera:Chironomidae) was studied and it was found that the range of the response was about $1.0 - 1.5\text{cm}$, not too far from our estimate. Similar measurements in mosquitoes (Diptera:Culicidae) show that the auditory perception range is about 2cm [36]. Of course, with this scatter of data, functional forms other than (4) can fit the susceptibility χ . However, given a phase transition scenario, data provides a physiologically reasonable estimate of the perception range in Diptera, which was far from trivial. This result seems a compelling support of the scaling scenario.

A percolation argument. There is an alternative way to estimate λ , which does not rely on the Vicsek model. Let us assume that the interaction between midges is step-like, being zero for distances larger than the perception range λ . This is a common assumption in most models of collective behaviour. We can then establish a link between each of the two insects closer than λ and calculate the size of the biggest cluster in the network. The larger λ , the larger this cluster. When the perception range exceeds the percolation threshold, $\lambda > \lambda_c$, a giant cluster of the same order as the group size appears [37]. We calculate the percolation threshold in swarms (see Methods) and find $\lambda_c = 1.67 r_1$. The crucial point is that varying the perception range λ at fixed nearest neighbour distance r_1 , is equivalent to varying r_1 at fixed λ . Hence, at fixed λ , there is an equivalent percolation threshold of the nearest neighbour distance, $(r_1)_c$, such that for $r_1 < (r_1)_c$ a giant cluster appears. Clearly, $(r_1)_c \sim \lambda/1.67$. Given a certain perception range λ , it is reasonable to hypothesize that the ordering transition in an interacting group occurs at values of the nearest neighbour distance close to the nearest neighbour percolation threshold, $(r_1)_c$. We conclude that $(r_1)_c \sim 0.60 \lambda$. This percolation argument therefore gives, $\lambda \sim 16 l - 19 l$, that is $\lambda \sim 2.0 - 4.5\text{cm}$, again quite consistent with the literature on the auditory perception range in Diptera.

This duality between r_1 and λ can be rephrased as follows. The perception range is close to the minimal value required to keep the network connected, given r_1 . A smaller perception range would cause the swarm to lose bulk connectivity. Equivalently, the critical nearest neighbour distance is close to the maximal distance compatible with a connected network, given λ . A sparser network would cause the swarm to lose bulk connectivity. Strictly speaking, the percolation argument only holds at equilibrium, because in a system where particles are self-propelled there may be order even at low density [26]. However, at low values of the noise, we still expect the percolation argument to give a reasonable, albeit crude, estimate of the perception range.

DISCUSSION

We have shown that natural swarms of midges lack collective order and yet display strong collective behaviour and correlation, similarly to what happens in ferromagnetic systems slightly above their critical point. Clusters of individuals that behave in a coordinated fashion and respond coherently to external stimuli grow with the group size. This, we believe, is the true signature of collective behaviour. In this perspective, the fact that a swarm does not move collectively, i.e. that it does not display emergent order, seems not to be a limitation of its collective capabilities, but rather a collective strategy, possibly related to the swarm mating purpose.

Swarms live in the scaling region at the edge of an ordering transition. As a consequence, swarms are effectively critical and have a collective response that is close to maximal. This is similar to what happens in bird flocks [21]. We say ‘effectively critical’ because if N is small, the ‘critical’ value of the rescaled nearest neighbour distance, $x_{\max}(N)$, can actually be quite far from the bulk critical point, x_c . What really matters is the balance between N and x , not just the vicinity of the control parameter to x_c . When dealing with animal groups, where N is never as large as in condensed matter systems, it is essential to keep in mind this finite size scaling description of criticality. It is the pair (x, N) to be apparently tuned to a sweet spot, which endows the group with a large collective response. It is hard to tell whether swarms tune the nearest neighbour distance to have enough response given their size, or whether a swarm grows to the maximum size sustainable at that given value of the nearest neighbour distance. In fact, it is unclear to us whether there is a way to distinguish between these two scenarios.

The presence of scaling effects in systems as different as bird flocks and insect swarms is intriguing [38]. After all, most physical systems are *not* at their critical point. But, at variance with physics, in biology a maximal collective response may give a significant evolutionary advantage. Living in the near-critical region may be an important condition to sustain collective behaviour in the most diverse biological systems.

Acknowledgments. We thank Enzo Branchini, Massimo Cencini and Francesco Ginelli for discussions. We also acknowledge the help of Tomas S. Grigera in running numerical tests on the single sample susceptibility in the Ising model. This work was supported by grants IIT–Seed Artswarm, ERC–StG n.257126 and US-AFOSR - FA95501010250 (through the University of Maryland).

Authors Contribution. A.C. and I.G. designed the study. A.C. coordinated the experiment. A.A., A.C., L.D.C., I.G., S.M., L.P., E.Shen and M.V. set up and calibrated the 3d system. L.D.C., S.M., O.P. and E.Shen performed the experiment. B.R. performed the species recognition and monitored all entomological aspects of the study. A.A., L.D.C., S.M., L.P.,

E. Shen, E.S. and M.V. performed the tracking and produced the $3d$ data. A.C., L.D.C., I.G., S.M., L.P. and M.V. analyzed the data. E.S. performed the numerical simulations. A.C. wrote the paper. Correspondence and requests for materials should be addressed to S.M. (stefania.melillo79@gmail.com) or A.C. (andrea.cavagna@roma1.infn.it).

METHODS

Experiments. Data was collected between May and October, in 2011 and in 2012, in the urban parks of Rome, at sunset. Midges are found near stagnant water. Swarms form above natural or artificial landmarks. Swarms have been video recorded under natural light. We acquired video sequences using a multi-camera system of three synchronized cameras (IDT-M5) shooting at 170 fps. Two cameras (the stereometric pair) were at a distance between 3m and 6m depending on the swarm and on the environmental constraints. A third camera, placed at a distance of 25cm from the first camera was used to solve tracking ambiguities. We used Schneider Xenoplan 50mm $f/2.0$ lenses. Typical exposure parameters: aperture $f/5.6$, exposure time 3ms. Recorded events have a time duration between 1.5 and 15.8 seconds. Swarm events of both Diptera:Ceratopogonidae and Diptera:Chironomidae were recorded. Among Chironomids, two different species were found (see SM-Table 1). To reconstruct the $3d$ positions and velocities of individual midges we used the techniques developed in [39]. Wind speed was recorded. After each acquisition we captured several midges in the recorded swarm for lab analysis.

Midge identification. Midges belonging to the family Chironomidae were identified to species according to [40], the ones belonging to the family Ceratopogonidae were identified according to [41] and [42]. Specimens used for identification were captured with a hand net and fixed in 70° alcohol, cleared and prepared according to [43]. Permanent slides were mounted in Canada Balsam and dissected according to [44].

Definition of the velocity fluctuations. To compute the correlation function we need to subtract from the velocity the contributions due to the collective motion. We identify three collective modes: translation, rotation and dilatation (expansion/contraction). Let $\{\vec{x}_i(t)\}$ be the coordinates of our system at time t . The position of the centre of mass is $\vec{x}_0(t) = 1/N \sum_i \vec{x}_i(t)$. We define the optimal translation as,

$$\Delta\vec{x}_T = \vec{x}_0(t + \Delta t) - \vec{x}_0(t). \quad (5)$$

We can now back-translate the coordinates, so that the centers of mass at two subsequent frames coincide, $\vec{y}_i(t) = \vec{x}_i(t) - \vec{x}_0(t)$. The optimal rotation is given by the

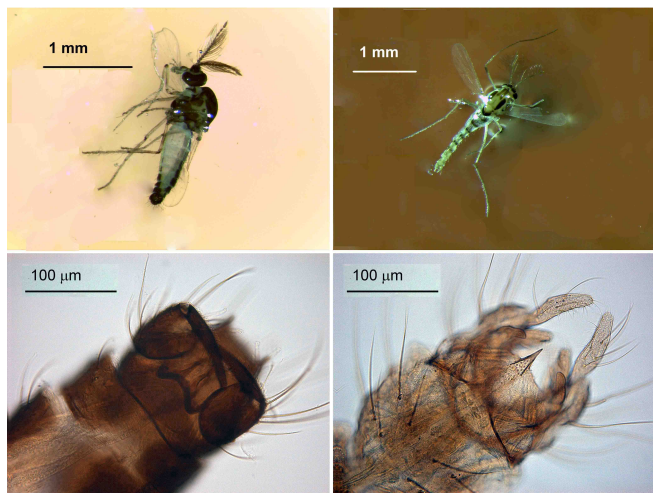


FIG. 4. Upper left: *Dasyhelea flavifrons* (Diptera:Ceratopogonidae), adult male. Lower left: male hypopygium of *D. flavifrons*. Upper right: *Cladotanytarsus atridorsum* (Diptera:Chironomidae), adult male. Lower right: male hypopygium of *C. atridorsum*.

3×3 orthogonal matrix R that minimizes the quantity,

$$\sum_i (\Delta\vec{y}_i)_R \equiv \sum_i [\vec{y}_i(t + \Delta t) - R\vec{y}_i(t)]^2.$$

The matrix R contains the information about the rotation axis, \hat{K} , and the rotation angle, θ . After having subtracted translation and rotation, we define the optimal dilatation as the scalar Λ which minimizes,

$$\sum_i (\Delta\vec{y}_i)_\Lambda \equiv \sum_i [R\vec{y}_i(t + \Delta t) - \Lambda R\vec{y}_i(t)]^2.$$

Both rotation and dilatation are computed using the Kabsch algorithm [45]. By subtracting the contribution of the three collective modes from the individual velocities we obtain the velocity fluctuation,

$$\delta\vec{v}_i = \vec{v}_i - \frac{1}{\Delta t} [\Delta\vec{x}_T + (\Delta\vec{y}_i)_R + (\Delta\vec{y}_i)_\Lambda]. \quad (6)$$

This is a dimensional quantity, hence it is impossible to compare the correlation of these fluctuations in different systems. We therefore introduce the dimensionless velocity fluctuation,

$$\delta\vec{\varphi}_i = \frac{\delta\vec{v}_i}{\sqrt{\frac{1}{N} \sum_k \vec{\delta}v_k \cdot \vec{\delta}v_k}}. \quad (7)$$

Rotation and dilatation order parameters. The rotational order parameter is defined as,

$$R = \frac{1}{N} \left| \sum_i \frac{\vec{y}_i^\perp(t) \times \vec{v}_i(t)}{|\vec{y}_i^\perp(t) \times \vec{v}_i(t)|} \cdot \hat{K} \right|, \quad (8)$$

where \vec{y}_i^\perp is the projection of $\vec{y}_i(t)$ on the plane orthogonal to the axis of rotation, the cross indicates a vectorial product, and \hat{K} is a unit vector in the direction of

the axis of rotation. In (8), $\vec{y}_i^\perp(t) \times \vec{v}_i(t)$ is the angular momentum of midge i with respect to the axis \hat{K} . In a perfectly coherent rotation all individuals would have angular momenta parallel to the axis, so that $R = 1$. In a noncoherent system, some of the projections of the angular momentum on \hat{K} would be positive and some negative, so $R \sim 0$. The dilatational order parameter is defined as,

$$\Lambda = \frac{1}{N} \sum_i \frac{[R \vec{y}_i(t)] \cdot [\vec{y}_i(t + \Delta t) - R \vec{y}_i(t)]}{|R \vec{y}_i(t)| |\vec{y}_i(t + \Delta t) - R \vec{y}_i(t)|}. \quad (9)$$

$\Lambda \in [-1, 1]$ and it measures the degree of coherent expansion (positive Λ) and contraction (negative Λ) of the swarm.

Noninteracting Harmonic Swarm. The NHS is an elementary model of non interacting particles performing a random walk in a three-dimensional harmonic potential. The dynamics of each particle is defined by the Langevin equation,

$$m \ddot{\vec{x}}_i(t) = -\gamma \dot{\vec{x}}_i(t) - k \vec{x}_i(t) + \sqrt{\eta \gamma} \vec{\xi}_i(t), \quad (10)$$

where $\vec{x}_i(t)$ is the position of the i -th particle at time t , m is the mass, γ the friction coefficient, k the harmonic constant and $\vec{\xi}_i(t)$ is a random vector with zero mean and unit variance, $\langle \xi_i^\alpha(t) \xi_j^\beta(t') \rangle = \delta(t - t') \delta_{i,j} \delta_{\alpha,\beta}$, with $\alpha = x, y, z$. The parameter η tunes the strength of the noise. The equation of motion are integrated with the Euler method [46]. We simulated the NHS in the critically damped regime ($\gamma^2 = 4mk$), which gives the best visual similarity to natural swarms. The number of particles N is set equal to that of the natural swarm we want to compare with. Parameters have been tuned to have a ratio between the distance traveled by a particle in one time step (frame) and the nearest neighbor distance comparable to natural swarms, $\Delta r / r_1 \sim 0.15$: $m = 1, k = 12.75, \gamma = 7.14, \eta = 2.0$.

Percolation threshold. For each frame we run a clustering algorithm with scale λ [47]: two points are connected when their distance is lower than λ . For each value of λ we compute the ratio n/N between the number of objects in the largest cluster and the total number of objects in the swarm (Fig.5). The percolation threshold, λ_c , is defined as the point where a giant cluster, i.e. a cluster with size of the same order as the entire system, forms [37]. We define λ_c as the point where $n/N = 0.6$. The percolation threshold scales with the nearest neighbour distance, $\lambda_c = 1.67 r_1$ (Fig.5, inset).

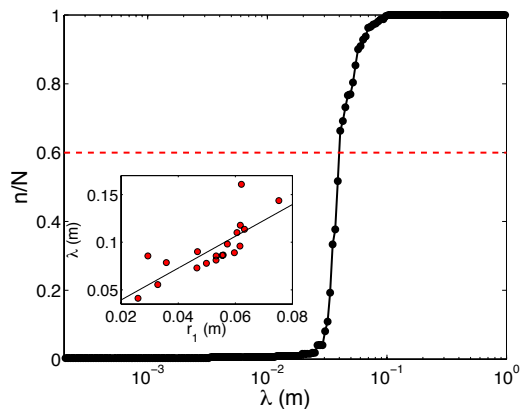


FIG. 5. **Percolation threshold.** Fraction of midges belonging to the largest cluster as a function of the clustering threshold λ . In correspondence of the percolation threshold λ_c there is the formation of a giant cluster. We define λ_c as the point where $n/N = 0.6$. This curve refers to event 20110909.3 and it is averaged over all time frames.

SUPPLEMENTARY INFORMATION

I. CONNECTED VS NONCONNECTED CORRELATION

The most basic kind of correlation one can measure is the scalar product of the velocities of individuals i and j , $\vec{v}_i \cdot \vec{v}_j$. This quantity is large if velocities are pointing in the same direction and low if they are uncorrelated. This is what is called *non-connected* correlation, and it has a problem: its value is trivially dominated by the *mean* motion of the system. Imagine that a gust of wind shifts the entire swarm, so that each midges's velocity is dominated by the wind speed. As an effect of the wind, midges i and j would be moving nearly parallel to each other, so that the non-connected correlation would be high. This, however, is simply an effect of the wind, and it is not a genuine sign of correlation, nor of interaction between the individuals. The same thing would happen in a system of uncorrelated particles put in rotational motion around an axis: velocities of nearby particle are mostly parallel as a mere effect of the overall rotation.

These examples show that we need to compute the correlation between the *fluctuations* around the mean motion of the system. In other words, what we want to detect is to what extent the individual changes of behaviour with respect to the global behaviour of the system are correlated. This is what the *connected* correlation does and it is the only reliable measure of correlation in a system. The presence of a non-connected correlation is not in general proof of anything at the level of the interaction, as the wind example clearly shows. On the other hand, the presence of non-zero connected correlation in a system is unambiguous proof that there is interaction, and strong enough to produce collective effects.

To compute the connected correlation function we must proceed as follows. First, we need to identify the collective modes of motion in the system and subtract them from the individual motion (see Methods). In this way we obtain the dimensionless fluctuations, $\delta\vec{\varphi}_i$, namely the velocity of midge i in a reference frame that not only is co-moving with the centre of mass, but also rotating and expanding/contracting as the whole swarm. Therefore, what is left is the deviation of i from the mean group motion, which is the only quantity that is safe to correlate. The connected correlation function is then defined as,

$$C(r) = \frac{\sum_{i \neq j}^N \delta\vec{\varphi}_i \cdot \delta\vec{\varphi}_j \delta(r - r_{ij})}{\sum_{i \neq j}^N \delta(r - r_{ij})}. \quad (11)$$

Unlike in [21] we do not normalize $C(r)$ by its value in $r \rightarrow 0$, because we want to compare the scale of correlation in the biological and synthetic case, so we must not amplify artificially the correlation signal.

It is very important to realize that an error or an artifact in computing the fluctuations can lead to spurious values of the correlation. As an example, consider two different and unrelated swarms moving in opposite directions, because of some weird fluctuation of the wind. If we fail to notice that these are *two* systems and analyze our data as if they were *one*, we get a zero net motion of the centre of mass. Hence, the velocity fluctuations are equal to the full velocities, and we are effectively computing a non-connected correlation, rather than a connected one, giving the delusion of very large correlation.

In the main text we show that swarms are mostly disordered. However, the fact that order parameters are low on average, does not mean that we can use the full velocities to compute the correlation function. As we have already said, a brief gust of wind can push the non-connected correlation function, to very high values. In this study, we are not investigating the origin of the order parameters fluctuations, but we focus on correlations. Hence, we have to be sure that correlation is computed in a way to avoid any spurious signal from the collective modes.

II. SUSCEPTIBILITY AS COLLECTIVE RESPONSE

In a stationary system, it can be proved [22] that the susceptibility is equal to the collective response of the system to uniform external perturbations. Maximum entropy calculations [48] show that the stationary probability distribution of the velocities in systems where there is an alignment interaction is given by,

$$P(v) = \frac{1}{Z} e^{J \sum_{i,j} \vec{v}_i \cdot \vec{v}_j}, \quad (12)$$

where J is the strength of the interaction (depending on distance r in a metric system) and Z is a normalizing

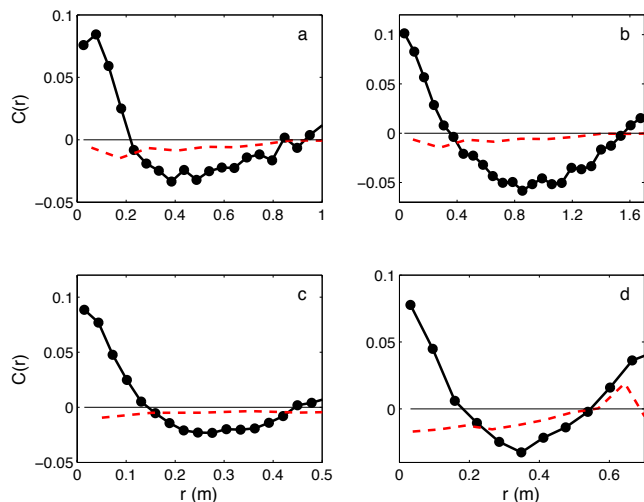


FIG. 6. **Connected correlation functions.** We present here the connected correlation function $C(r)$ in four of our swarms, different from the one in the main text. All correlation functions are averaged in time. **a:** Swarm 20120910_A1 - CA; **b:** Swarm 20120907_A1 - CA; **c:** Swarm 20110909_A3 - CS; **d:** Swarm 20120702_A2 - DF;

factor (the partition function),

$$Z = \int Dv e^{J \sum_{i,j} \vec{v}_i \cdot \vec{v}_j}. \quad (13)$$

If an external perturbation (or field) h couples uniformly to all velocities, this distribution gets modified as,

$$P(v) = \frac{1}{Z(h)} e^{J \sum_{i,j} \vec{v}_i \cdot \vec{v}_j + \vec{h} \cdot \sum_i \vec{v}_i}. \quad (14)$$

Now we ask what is the collective response χ of the system to a small variation of the perturbation h . To answer this question we calculate the variation of the global order parameter, i.e. of the space average of the velocity, under a small variation of h . we have,

$$\begin{aligned} \chi &= \frac{\partial}{\partial h} \left\langle \frac{1}{N} \sum_k v_k \right\rangle \\ &= \frac{\partial}{\partial h} \int Dv P(v) \frac{1}{N} \sum_k v_k \\ &= \frac{1}{N} \sum_{i,k} \int Dv P(v) v_k v_i - \int Dv P(v) v_i \int Dv P(v) v_k \\ &= \frac{1}{N} \sum_{i,k} \langle v_k v_i \rangle - \langle v_i \rangle \langle v_k \rangle = \frac{1}{N} \sum_{i,k} \langle \delta v_k \delta v_i \rangle, \end{aligned} \quad (15)$$

where we have disregarded the vectorial nature of the quantities not to burden the notation and where we have defined,

$$\langle f(v) \rangle = \int Dv P(v) f(v). \quad (16)$$

Apart from the missing normalization, needed to make χ dimensionless, the quantity in (15) is exactly the susceptibility defined in the main text, equation (2).

III. SIMULATIONS OF THE VICSEK MODEL IN THREE DIMENSIONS

We performed numerical simulations of the metric Vicsek model in $3d$ [25–27]. In this model each particle tends to align its direction of motion to that of its metric neighbours. More precisely, the direction of particle i at time $t + 1$ is the average direction of all particles within a sphere of radius λ around i (including i itself). The parameter λ is therefore the metric radius of interaction, that is the perception range. The resulting direction of motion is then perturbed with a random rotation, playing the role of noise. Particles have all fixed velocity modulus $|\vec{v}| = v_0$. The update equation of the model is,

$$\vec{v}_i(t+1) = v_0 \mathcal{R}_\eta \left[\Theta \left(\sum_{j \in S_i} \vec{v}_j(t) \right) \right], \quad (17)$$

where S_i is the spherical neighborhood of radius λ centered around i , Θ is the normalization operator $\Theta(\vec{x}) = \vec{x}/|\vec{x}|$ and \mathcal{R}_η performs a random rotation uniformly distributed around the argument vector with maximum amplitude of $4\pi\eta$. The position r_i is updated with the following rule,

$$\vec{r}_i(t+1) = \vec{r}_i(t) + \vec{v}_i(t+1). \quad (18)$$

Particles move in a cubic box with periodic boundary conditions. Note that if we wanted to reproduce in the simulation the cohesion of natural swarms, we do not need to introduce an inter-individual attraction force, but simply an external harmonic potential equal for all particles [4, 16, 20]. This is the simplest way to reproduce cohesion in natural swarms, which are known to keep their average position with reference to a visual marker [13]. This is a crucial difference with bird flocks, where cohesion must be enforced with an inter-individual force.

The control parameter of interest for us is $x \equiv r_1/\lambda$, where r_1 is the nearest neighbour distance, which we can tune by changing the density. In the Vicsek model there is a transition from a disordered to an ordered phase when decreasing x . We studied the susceptibility $\chi(x, N)$ for different system sizes $N \in [128, 8192]$, and different values of $x \in [0.34, 0.70]$. The particles velocity is, $v_0 = 0.05$. Each simulation has a duration of 6×10^5 time steps, with initial conditions consisting in uniformly distributed positions in the cubic box and uniformly distributed directions in the 4π solid angle. After a transient of 10^5 time steps, we saved 500 configurations at intervals of 1000 time steps in order to have configurations with velocity fluctuations uncorrelated in time.

A crucial parameter is the value of the noise, η , because the position of the critical point x_c depends on η [25–27]. Given that we want establish a connection between the critical point of Vicsek and that of natural swarms, we need some calibration. To do this, we run simulations at several noise values, and chose the value of η that makes the maximum susceptibility as a function of N as close as possible to that of swarms (this kind of calibration is made possible by the fact that χ is a dimensionless quantity). We find that this happens at $\eta = 0.45$, where we find $x_c = 0.43$. Other values of the noise give: $\eta = 0.40, x_c = 0.45$; $\eta = 0.35, x_c = 0.47$. At this last value of η the Vicsek susceptibility is way larger than that of the swarms. Hence, the error in the calibration of the critical point seems limited: we may be off at most by 10%.

Several numerical analysis have been performed on the critical behaviour of the Vicsek model. Most works focus on the two dimensional case [25, 27, 34], where an exhaustive exploration of the parameters space is possible. Some more recent analysis also treat the computationally more demanding case of three dimensions [26, 27, 49]. For what concerns the nature of the ordering transition, it has been shown that in the thermodynamic limit (and with metric interaction), the transition in the Vicsek model is first order [27]. However, it has also been shown that, unless N is much larger than the values analyzed here, the transition is indistinguishable from a second order one [25, 27], and scaling theory well describes the behaviour around the critical point [34].

IV. SUSCEPTIBILITY AND SCALING RELATIONS

Here we analyze in detail the relation between correlation function and susceptibility. From equations (1) and (2), we obtain:

$$Q(r) = \frac{1}{N} \int_0^r dr' \sum_{i \neq j} \delta(r' - r_{ij}) C(r'). \quad (19)$$

If we make the hypothesis that mass fluctuations are not strong, we can write,

$$\frac{1}{N} \sum_{i \neq j} \delta(r' - r_{ij}) \sim 4\pi x^2 \rho, \quad (20)$$

where ρ is the density. Hence, we get,

$$Q(r) = \frac{3}{r_1^3} \int_0^r dr' r'^2 C(r'). \quad (21)$$

where we have used the simple relationship between density and nearest neighbours distance, $4\pi\rho = 3/r_1^3$. In an infinitely large system, the bulk susceptibility is simply, $\chi_\infty = Q(r \rightarrow \infty)$, that is the full volume integral of the connected correlation function. In a finite size system,

however, due to the constraint, $\sum_i \delta\vec{\varphi}_i = 0$, we must have $Q(r=L) = -1$. In this case the susceptibility can be estimated as the maximum value reached by $Q(r)$ (this maximum is a lower bound for the bulk susceptibility). We know that, $C(r_0) = 0$, so that the function $Q(r)$ reaches its maximum at $r = r_0$. Hence the finite size susceptibility is given by,

$$\chi = Q(r_0) = \frac{3}{r_1^3} \int_0^{r_0} dr r^2 C(r). \quad (22)$$

To proceed we need to know more about r_0 . In a system with finite size L , we have,

$$C(r) = G(r) - \frac{3}{L^3} \int_0^L dr r^2 G(r), \quad (23)$$

where $G(r)$ is the *bulk* correlation function, i.e. the correlation function in an infinitely large system. The equation $C(r_0) = 0$ therefore gives,

$$G(r_0) = \frac{3}{L^3} \int_0^L dr r^2 G(r), \quad (24)$$

and the finite size susceptibility becomes,

$$\chi = \frac{3}{r_1^3} \int_0^{r_0} dr r^2 G(r) - \frac{3r_0^3}{r_1^3 L^3} \int_0^L dr r^2 G(r). \quad (25)$$

In the scaling region, we have that the correlation function has a scale-free form,

$$G(r) = \left(\frac{\lambda}{r}\right)^\alpha, \quad (26)$$

where λ is the range of the interaction, making the correlation function dimensionless. The exponent α is normally quite close to $d - 1$; in the equilibrium theory of critical phenomena $\alpha = d - 2 + \eta$ and typically $0 \leq \eta \leq 0.1$, hence $\alpha \sim 1$ in three dimensions. However, in off-equilibrium systems there are deviations from the critical prediction [25, 50] and in bird flocks it has been found $\alpha \ll 1$ [21, 51]. From (24) and (26) we get that in the scaling region the correlation length scales with the system's linear size,

$$r_0 \sim L. \quad (27)$$

This happens both in bird flocks [21] and in swarms (Fig.2d). From (25) we finally obtain the susceptibility in the scaling region,

$$\chi(N) \sim \frac{\lambda^\alpha L^{3-\alpha}}{r_1^3} = \frac{1}{x^\alpha} N^{1-\alpha/3}, \quad (28)$$

where, as in the main text, we have defined $x \equiv r_1/\lambda$. In a system with topological interaction everything must be invariant under rescaling of the nearest neighbour distance r_1 , hence $\lambda \sim r_1$, as it happens in bird flocks [24] and so the prefactor in (28) is of order 1. In this case (28)

is equivalent to the standard finite size scaling relation, $\chi \sim L^{\gamma/\nu}$ of critical phenomena [2, 22].

In a metric system, on the other hand, r_c does not scale with r_1 , hence the factor $1/x^\alpha$ remains in (28). In the scaling region we have that,

$$x \sim x_{\max}(N) \sim x_c + \frac{1}{N^{1/3\nu}} \quad (29)$$

where ν is one of the critical exponents [22]. This decrease of x with N is verified in swarms (Fig.7), supporting the hypothesis that swarms are in the scaling regime. If we plug (29) into (28) we do not get an exact power law behaviour of χ vs. N . However, the practical effect on the data is to see a power law,

$$\chi(N) \sim N^\beta, \quad (30)$$

with an exponent β slightly larger than $1 - \alpha/3$. We conclude that in the near critical regime the susceptibility grows like the number of individuals to a power quite close to 1. This is indeed what we find in the swarm data (Fig.2c).

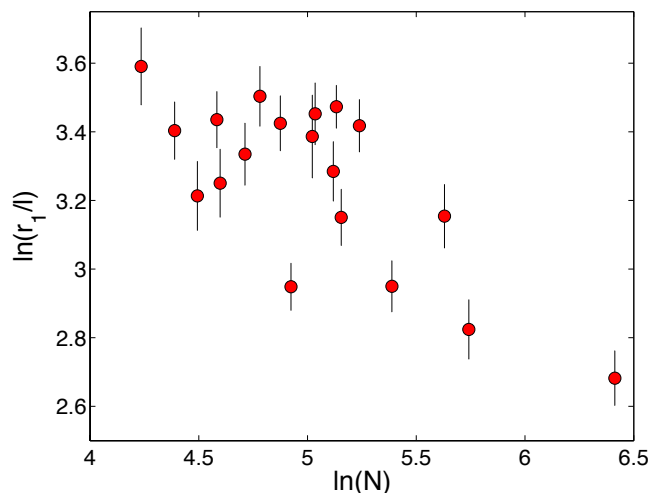


FIG. 7. **Scaling regime.** In the scaling regime the control parameter x must decrease with the system size N . In swarms the control parameter is r_1/l , nearest neighbour distance over body length, which we plot here vs. N . The signature of the scaling regime is quite clear.

SPECIES	EVENT LABEL	N	DURATION (s)	$r_1(m)$	$r_0(m)$	χ	ϕ
<i>Corynoneura scutellata</i> - CS (Diptera:Chironomidae)	20110906_A3	138	2.0	0.029	0.094	0.78	0.17
	20110908_A1	119	4.4	0.036	0.105	0.46	0.27
	20110909_A3	312	2.7	0.026	0.138	2.58	0.22
<i>Cladotanytarsus atridorsum</i> - CA (Diptera:Chironomidae)	20110930_A1	173	5.9	0.057	0.228	1.48	0.31
	20110930_A2	99	5.9	0.063	0.223	1.08	0.20
	20111011_A1	131	5.9	0.075	0.272	0.65	0.17
	20120828_A1	89	6.3	0.062	0.188	0.48	0.22
	20120907_A1	169	3.2	0.062	0.330	1.72	0.20
	20120910_A1	219	1.7	0.047	0.221	2.25	0.27
	20120917_A3	610	1.5	0.033	0.252	9.30	0.20
	20120918_A2	69	15.8	0.060	0.174	0.64	0.23
<i>Dasyhelea flavifrons</i> - DF (Diptera:Ceratopogonidae)	20110511_A2	279	0.9	0.053	0.248	1.25	0.35
	20120702_A1	98	2.1	0.062	0.162	0.69	0.20
	20120702_A2	111	7.3	0.056	0.169	0.88	0.18
	20120702_A3	80	10.0	0.060	0.170	0.32	0.20
	20120703_A2	167	4.4	0.046	0.140	0.52	0.12
	20120704_A1	152	10.0	0.050	0.154	0.63	0.15
	20120704_A2	154	5.3	0.053	0.160	0.61	0.13
	20120705_A1	188	5.9	0.055	0.182	0.92	0.20

TABLE I. **Swarm data.** Each line represents a different swarming event (acquisition). N is the number of individuals in the swarm, r_1 the time average nearest neighbour distance in the particular acquisition, r_0 the average correlation length, χ the average susceptibility and ϕ the average polarization.

-
- [1] Krause, J. and Ruxton, G. D. *Living in Groups* (Oxford University Press, Oxford, 2002).
- [2] Cardy, J. *Scaling and Renormalization in Statistical Physics* (Cambridge Lecture Notes in Physics, Cambridge University Press, Cambridge, 1996)
- [3] Parisi G, *Statistical Field Theory* (Westview Press, 1998)
- [4] Okubo A Dynamical aspects of animal grouping: Swarms, schools, flocks, and herds *Adv. Biophys.* **22**, 1-94 (1986).
- [5] Camazine, S., Deneubourg, J.-L., Franks, N. R., Sneyd, J., Theraulaz, G., and Bonabeau, E. *Self-Organization in Biological Systems* (Princeton University Press, Princeton, 2003)
- [6] Sumpter, D.J.T. *Collective Animal Behavior* (Princeton University Press, Princeton 2010)
- [7] Downes, J. A. The swarming and mating flight of Diptera. *Ann. Rev. Entomol.* **14** (1969): 271-298.
- [8] Sullivan RT, Insect swarming and mating, *Florida Entomol.* **64**, 44–65 (1981).
- [9] Nielsen, E.T., Haeger, J.S. Swarming and mating in mosquitoes. *Miscell. Publ. Entomol. Soc. Am.* **1**, 7295 (1960)
- [10] Charlwood JD, Jones MDR. Mating in the mosquito *Anopheles gambiae* sl. 2. swarming behavior. *Physiol. Entomol.* **5**, 315320. (1980).
- [11] Manoukis, N. C., Diabate, A., Abdoulaye, A., Diallo, M., Dao, A. Structure and dynamics of male swarms of *Anopheles gambiae*. *J. Med. Entomol.* **46**, 227–235 (2009).
- [12] Okubo, A., Grunbaum, D., & Edelstein-Keshet, L. (2001). The dynamics of animal grouping. *Interdiscip. Appl. Math*
- [13] Downes, J. A. "Observations on the swarming flight and mating of *Culicoides* (Diptera: Ceratopogonidae) 1." *Transactions of the Royal Entomological Society of London* 106.5 (1955): 213-236.
- [14] Blackwell, A., Mordue (Luntz), A. J., Mordue, W. The swarming behaviour of the Scottish biting midge, *Culicoides impunctatus* (Diptera: Ceratopogonidae) *Ecol. Entomol.* **17**, 319–325 (1992)
- [15] Okubo, A., Chiang, H.C. An analysis of the kinematics of swarming of *Anarete Prithcardi Kim* (Diptera: Cecidomyiidae), *Res. Popul. Ecol.* **16**, 1–42 (1974)
- [16] Butail, S., Manoukis, N. C., Diallo, M., Ribeiro, J. M., & Paley, D. A. The Dance of Male *Anopheles gambiae* in Wild Mating Swarms. *J. Med. Entomol.* **50**, 552-559 (2013).
- [17] Ali, A., Nuisance chironomids and their control: a review. *Bulletin of the ESA* **26**, 3 (1980).
- [18] Rose, R. I., Pesticides and public health: integrated methods of mosquito management. *Emerging Infectious Diseases* **7**, 17 (2001).
- [19] Shinn, E. A., & Long, G. E. Technique for 3-D analysis of *Cheumatopsyche pettiti* (Trichoptera: Hydropsychidae) swarms. *Environ. Entomol.* **15**, 355-359 (1986).
- [20] Kelley, D. H., & Ouellette, N. T. Emergent dynamics of laboratory insect swarms. *Scientific Reports* **3**, 1073 (2013).

- [21] Cavagna, A., Cimarelli, A., Giardina, I., Parisi, G., Santagati, R., Stefanini, F., and Viale, M. Scale-free correlations in starling flocks *Proc. Natl. Acad. Sci. USA* **107**, 11865–11870 (2010)
- [22] Binney, J. J., Dowrick, N. J., Fisher, A. J., & Newman, M. *The theory of critical phenomena: an introduction to the renormalization group*. (Oxford University Press, Oxford, 1992)
- [23] Huang, K. *Statistical Mechanics*. (Wiley, John & Sons, New York, 1990)
- [24] Ballerini, M., Cabibbo, N., Candelier, R., Cavagna, A., Cisbani, E., Giardina, I., Lecomte, V., Orlandi, A., Parisi, G., Procaccini, A., et al. Interaction ruling animal collective behavior depends on topological rather than metric distance: Evidence from a field study *Proc. Natl. Acad. Sci. USA* **105**, 1232–1237 (2008).
- [25] Vicsek, T., Czirók, A., Ben-Jacob, E., Cohen, I., and Shochet, O. Novel type of phase transition in a system of self-driven particles *Phys. Rev. Lett.* **75**, 1226–1229 (1995).
- [26] Gonci, B., Nagy, M., & Vicsek, T.. Phase transition in the scalar noise model of collective motion in three dimensions. *Europ. Phys. J. Special Topics* **157**, 53-59 (2008).
- [27] Chaté, H., Ginelli, F., Grégoire, G., & Raynaud, F. Collective motion of self-propelled particles interacting without cohesion. *Phys. Rev. E* **77**, 046113 (2008).
- [28] Couzin, I. D., Krause, J., James, R., Ruxton, G. D., and Franks, N. R. Collective memory and spatial sorting in animal groups *J. Theor. Biol.* **218**, 1–11 (2002)
- [29] Buhl, J., Sumpter, D. J. T., Couzin, I. D., Hale, J. J., Despland, E., Miller, E. R., & Simpson, S. J. From disorder to order in marching locusts. *Science* **312**, 1402-1406 (2006).
- [30] Becco, C., Vandewalle, N., Delcourt, J. and Poncin, P. Experimental evidences of a structural and dynamical transition in fish school, *Physica A* **367** 487–493 (2006)
- [31] Makris NC, Ratilal P, Symonds DT, Jagannathan S, Lee S, Nero RW. Critical population density triggers rapid formation of vast oceanic fish shoals. *Science* **311**, 660-663 (2006).
- [32] *Finite Size Scaling and Numerical Simulations of Statistical Systems*, edited by V. Privman (World Scientific, Singapore, 1990).
- [33] Sides, S.W., Rikvold, P. A. and Novotny, M. A., Kinetic Ising model in an oscillating field: Finite-size scaling at the dynamic phase transition, *Phys. Rev. Lett.* **81**, 834 (1998).
- [34] Baglietto, G. & Albano, E.V. Finite-size scaling analysis and dynamic study of the critical behavior of a model for the collective displacement of self-driven individuals *Phys. Rev. E* **78**, 021125 (2008).
- [35] Fyodorova, M. V., & Azovsky, A. I. Interactions between swarming *Chironomus annularius* (Diptera: Chironomidae) males: role of acoustic behavior. *J. Insect Behav.* **16**, 295-306 (2003).
- [36] Pernetier, C., Warren, B., Dabiré, K. R., Russell, I. J., & Gibson, G. "Singing on the Wing as a Mechanism for Species Recognition in the Malarial Mosquito *Anopheles gambiae* *Current Biology* **20**, 131-136 (2010)
- [37] Kertesz, J., Stauffer, D., & Coniglio, A. in: Deutcher, G.D. Zallen, J., Adles, J. Eds. *Percolation Structures and Processes* (Adam Hilger, Bristol, 1983)
- [38] Bialek W. & Mora T., Are biological systems poised at criticality? *J. Stat. Phys.* **144**, 268-302 (2011)
- [39] Attanasi, A., Cavagna, A., Del Castello, L., Giardina, I., Jelic, A., Melillo, S., Parisi, L., Shen, E., Silvestri, E. & Viale, M. (2013). Tracking in three dimensions via multi-path branching. *preprint* arXiv:1305.1495.
- [40] Langton P. H. & Pinder L. C. V. Keys to the adult male chironomidae of Britain and Ireland Vol I, Vol II, (SP 64, The Freshwater Biological Association, Ambleside, 2007).
- [41] Kieffer J. J. Faune de France, Vol. 11: Diptères Nématocères Piqueurs: Chironomidae, Ceratopogoninae (Lechevalier, Paris, 1925).
- [42] Dominiak P. Biting midges of the genus *Dasyhelea* Kieffer (Diptera: Ceratopogonidae) *Poland Polish Journal of Entomology* **81**, 211-304 (2012).
- [43] Wirth W.W., & Marston N. A method for mounting small insects on microscope slides in Canada balsam. *Annals of the Entomological Society of America* **61**, 783-784 (1968).
- [44] Wiederholm T. Chironomidae of the Holarctic Region . Keys and Diagnoses. Part III. Adult males. *Entomologica Scandinavica Suppl.* **34**, 1-532 (1989).
- [45] Kabsch, W. A solution for the best rotation to relate two sets of vectors. *Acta Crystallographica* **32**, 922–923 (1976).
- [46] Butcher, J.C. *Numerical Methods for Ordinary Differential Equations* (John Wiley & Sons, New York, 2003)
- [47] Lu, S. Y. and Fu, K. S. 1978. A sentence-to-sentence clustering procedure for pattern analysis. *IEEE Trans. Syst. Man Cybern.* 8,381389.
- [48] Bialek, W., Cavagna, A., Giardina, I., Mora, T., Silvestri, E., Viale, M., & Walczak, A. M. Statistical mechanics for natural flocks of birds. *Proc. Natl. Acad. Sci. USA* **109**, 4786-4791 (2012).
- [49] Czirok, A., Vicsek, M. & Vicsek, T. Collective motion of organisms in three dimensions. *Physica A* **264**, 299-304 (1999).
- [50] Toner, J. and Tu, Y. Flocks, herds, and schools: A quantitative theory of flocking *Phys. Rev. E* **58**, 4828–4858 (1998)
- [51] Cavagna, A., Giardina, I., Ginelli, F. Boundary information inflow enhances correlation in flocking. *Phys. Rev. Lett.* **110**, 168107.